Earthquake forecasting model for Albania: the area source model and the smoothing model

Edlira Xhafaj[1,2,3], Chung-Han Chan[3,4], Kuo-Fong Ma[1,2,3]

[1]Taiwan International Graduate Program (TIGP)–Earth System Science Program, Academia Sinica and National Central University, Academia Sinica, Taipei 11529, Taiwan
[2]Institute of Earth Sciences, Academia Sinica, Taipei 11529, Taiwan
[3]Earthquake-Disaster & Risk Evaluation and Management (E-DREaM) Center, National Central University, Taoyuan, 32001, Taiwan
[4]Department of Earth Sciences, National Central University, Taoyuan, 32001, Taiwan

Correspondence to: Chung-Han Chan (hantijun@googlemail.com)

Abstract. We proposed earthquake forecasting models for Albania, one of the most seismogenic regions in Europe, to give an overview of seismic activity by implementing area source and smoothing approaches. The earthquake catalog was first declustered to remove foreshocks and aftershocks when they were within the derived distance and time windows of mainshocks. Considering catalog completeness, the events with M≥4.0 during the period of 1960 – 2006 were implemented for the forecast model learning. The forecasting is implemented into an area source model that includes 20 sub-regions and a smoothing model with a cell size of 0.2˚ x 0.2˚ to forecast the seismicity in Albania. Both models show high seismic rates along the western coastline and in the southern part of the study area, which is consistent with previous studies that discussed seismicity in the area and currently active regions. To further validate the forecast performance from the two models, we introduced the Molchan diagram to quantify the correlation between models and observations. The Molchan diagram suggests that both models are significantly better than a random distribution, confirming their forecasting abilities. Our results provide crucial information for subsequent research on seismic activity, such as probabilistic seismic hazard assessment.

1 Introduction

Albania located in Balkan Peninsula belongs to the Alpine-Mediterranean seismic belt, one of the most seismic regions in Europe often threatened by devastating earthquakes, along with Turkey and Greece (Aliaj et al., 2010; Sulstarova, 1996). High seismicity activity in the region has been the main scope of many researches from Albanian and other experts, which include Albania as part of their seismic hazard analysis (e.g., Shebalin et al., 1974; Sulstarova, 1996; Slejko et al., 1999; Aliaj et al., 2004; Aliaj et al., 2010; Fundo et al., 2012; Muco et al., 2012), multinational programs and projects within Europe, Balkan and the Mediterranean region (e.g., Giardini, 1999; Jiménez et al., 2001; Jimenez et al., 2003; Woessner, et al., 2015; Salic et al., 2018). So far, however, no controlled studies in Albania put attention to the correlation between seismic models for Albania. There are two primary aims of this study: (1) to investigate the earthquake forecasting in Albania from different models, and, (2) to assure the credibility of these models. We focus on the seismic activity considering shallow crust events, which for the

Albania case are generally with depth at 10-20 km and, in many cases, near the surface (Sulstarova, 1996). The Albanian Seismological Network (ASN) data regarding the events from 1976 to 2000 show that 95% of earthquakes had depths of less than 30 km (Muco et al., 2002). We investigate the seismicity of events that occurred in the region during period of time 1960 to 2006, from the 2013 European Seismic Hazard Model (ESHM13) in the framework of the Seismic Hazard Harmonization in Europe project (referred to as SHARE), based on the SHARE European Earthquake Catalogue (SHEEC). By analyzing the catalog, we aim to propose earthquake forecasting models, which can be used for future research works to understand the seismicity in area and compare with models that include extended catalog, seismogenic sources which are not incorporated into our forecasting model. The time period of 46 years was chosen after the catalog is declustered according to the Gardner and Knopoff (1974) window method to evaluate the completeness time, threshold magnitude, and Gutenberg-Richter parameters (Gutenberg and Richter, 1944). Based on the catalog, we could forecast the Albanian seismicity by implementing two models, the standard Cornell (1968) approach based on the area source model and the smoothing model by Frankel (1995). Area source polygons are defined by the ESHM13, designed with the assumption that seismicity may occur anywhere within each zone, and delineation considers seismicity, tectonics, geology, and geodesy (Woessner et al., 2015). To avoid subjective judgments regarding how area sources polygons are designed, a smoothing model is an alternative approach used to forecast seismicity. The method is based on the principle that the distribution of past events can be used to predict where future events may occur (Frankel, 1995).

Both models demonstrate/perform a high seismic rate along the western coastline and south part of the study area, consistent with previous studies and currently active regions. To further evaluate the forecasting results from two models, we introduced the Molchan diagram to investigate the correlation between models and observations. The catalog from 1960 to 2006 is regarded as the "learning period" for model construction, and the seismicity during 2015-2020 is the "testing period" for comparing and validating the results. In addition, the null hypothesis is applied to confirm the forecasting ability of the models and the results are performed for events according to each of the threshold magnitudes, which confirm good forecasting ability of both models. Finally, the results obtained from comparing learning and testing period are presented and discussed.

2 Earthquake catalog and analyzes

2.1 Catalog dataset

To analyze the seismicity, our area of study is bounded between the latitude of 38.0ºN-44.5ºN and the longitude of 18.0ºE-23.0ºE (Fig.1), and a seismicity working file is created for further analysis. The SHEEC catalog during 1900 and 2006 was compiled by the German Research Center for Geo-sciences (GFZ, Potsdam) and released as part of an independent project, representing a spatial-temporal extract from the "European-Mediterranean Earthquake Catalogue (EMEC, Grünthal and Wahlström, 2012; Grünthal et al., 2013)", which contains seismic events with moment magnitude from 3.5 to 7.0 for our region of study. We implemented the events with depth ≤ 35 km, considered as shallow crustal events, according to previous studies (Muço, 1998; Slejko et al., 1999; Muco et al., 2002; Aliaj et al., 2004), and the ESHM13 (Woessner et al., 2015). The catalog

from 1900-2006 is considered to obtain completeness intervals for the entire study region using the cumulative number of events over time (Fig.1a).
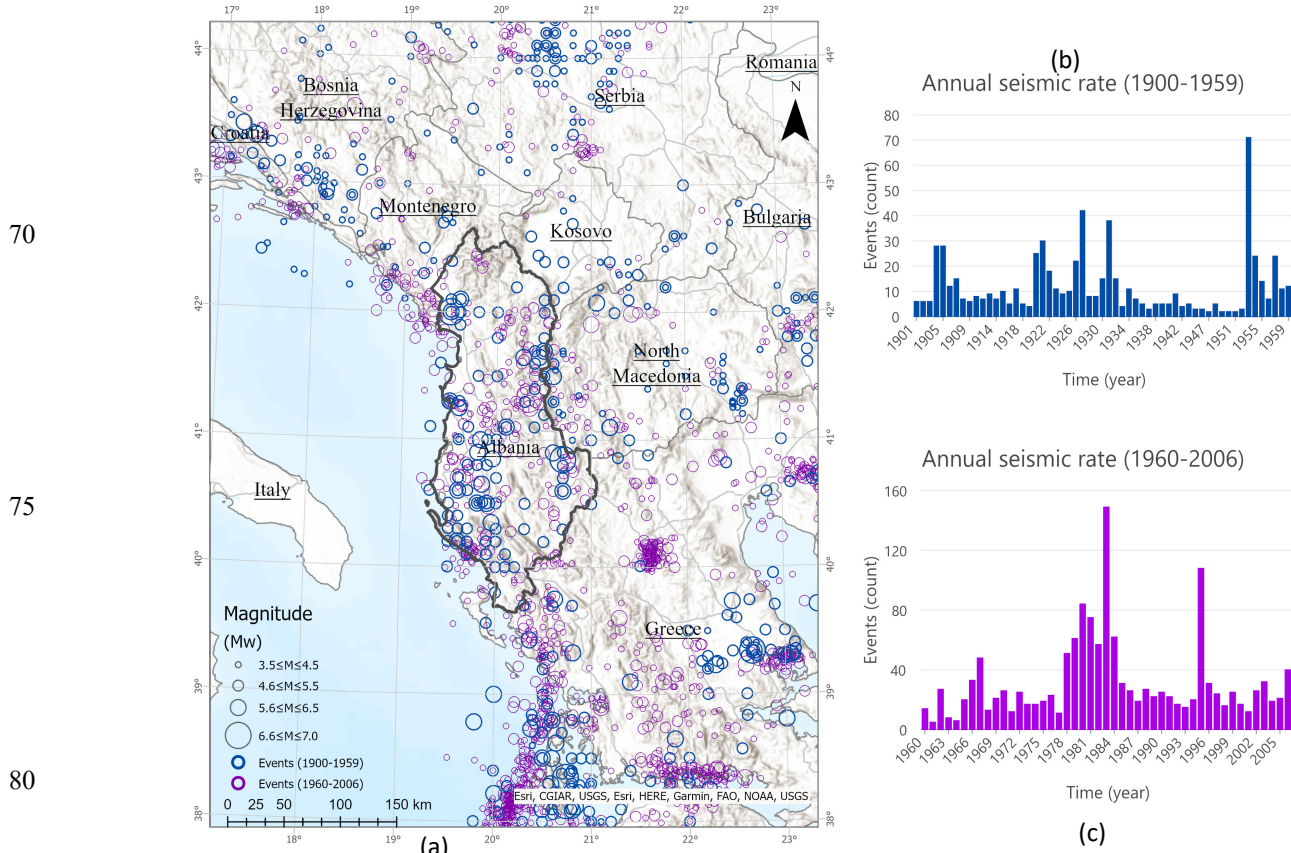
Figure 1: a) Map of epicenters of all the shallow earthquakes (depth ≤ 35 km) with magnitude Mw ≥ 3.5 for the period of time 1900-1959 represented by blue circles and the period 1960-2006 represented by purple circles. b) Annual seismic rate for the non-declustered catalog with all the events that occurred during the period 1900-1959, and c) annual seismic rate for the non-declustered catalog with all the events that occurred during the period 1960-2006. The size of the circles corresponds to the magnitude of the earthquake.

When the slope changes we consider the catalog as completed for the magnitudes above reference (Duni et al., 2010; Markus et al., 2016), also consistent with the intervals obtained from applying the Stepp (1972) approach. The completeness intervals for the selected area are identified with magnitude threshold 4.1 for the period 1974-2006, completed events with magnitude 4.5 and 5.0 after 1950 and 1901, respectively. Duni et al. (2010) and Makropoulos et al. (2012) have reported similar completeness intervals. Further analysis on this study focused on the period of time between 1960 to 2006 (Fig.2), a period during which catalog is more complete and mainly based on instrumental data during the 20th century (Çağnan and Kalafat et al., 2012; Markušić et al., 2016).
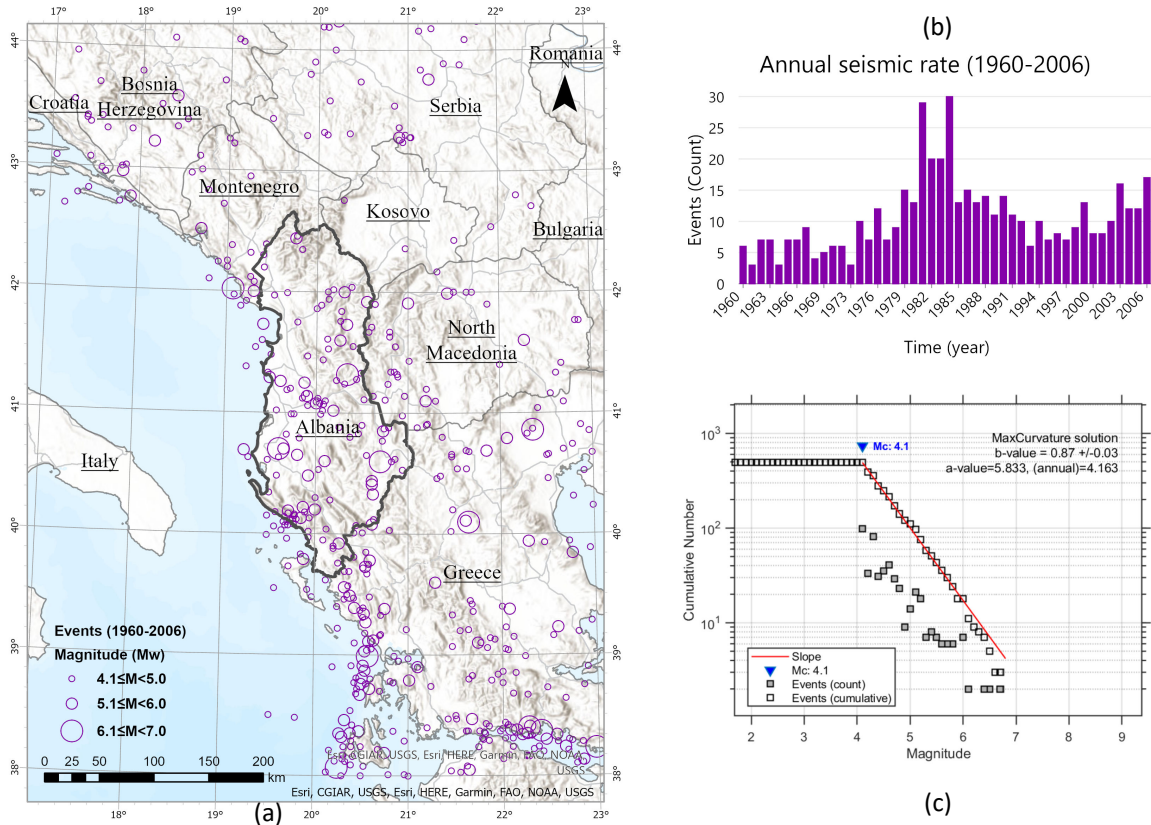
Figure 2: a) Distribution of declustered events with a magnitude larger than 4.1 occurred from 1960 to 2006. b) The annual seismic rate for the events that occurred during the period 1960–2006; and, c) the magnitude of completeness from the declustered catalog.

2.2 Catalog declustering

115   Declustering earthquake catalog is a standard procedure for seismicity modeling to keep only the mainshocks (the largest events in an earthquake sequence), removing events identified as foreshocks and aftershocks in a space-time window. The method is commonly used in engineering seismology and statistical seismology, e.g., probabilistic seismic hazard assessment and earthquake forecasting. A variety of techniques for declustering a catalog to obtain background seismicity have been proposed, the majority of these methods eliminate earthquakes in a space-time window following a large occurrence known

120   as the mainshock (Zhuang et al., 2002). The Gardner and Knopoff method (Gardner and Knopoff, 1974, also known as GK-1974) describes space-time windows dependent on the magnitude of the mainshock and denotes events inside the window of a large event as foreshocks or aftershocks. The space- and time-windows of the GK-1974 produce a declustered catalog that follows a Poisson distribution, which is not seen in other declustering methods (van Stiphout et al., 2012), and they present as:

$$L(km) = 10^{0.1238*M+0.983} , \quad T(days) = \begin{cases} 10^{0.5409*M-0.547}, & if M < 6.5 \\ 10^{0.032*M+2.7389}, & if M \geq 6.5 \end{cases}, \text{respectively,} \quad (1)$$

where M is the magnitude of the mainshock, L is the distance from the mainshock in kilometers, and T is the time in days. Given the moment magnitude of each earthquake in our catalog, using the algorithms from GK-1974, we calculated a specific distance L(M) and time T(M) to denote the foreshock and aftershock that take place before and after the mainshock, respectively. All the events are sorted according to their magnitudes (highest to lowest), and those events that are within the spatial and temporal window of large events are dependent. Our forecasting models are conducted using only mainshocks, as considering dependent events (foreshocks and aftershocks) would lead to a higher seismicity rate (e.g., Chan et al., 2016).

2.3 The magnitude of completeness (Mc)

The magnitude of completeness is defined as the minimum magnitude above which all earthquakes are reliably recorded, and the value varies over time and space. Mc could be estimated based on the Gutenberg-Richter Law (Gutenberg and Richter, 1944), classifying earthquakes by the number of occurrences with magnitudes greater than a given reference magnitude. Magnitude-frequency relation, the Gutenberg-Richter Law is performed as:

$$logN(M) = a - b * M , \hspace{3cm} (2)$$

where N(M) is the number of earthquakes per year for a magnitude equal to M or larger than M, a-value (activity rate) represents the total seismic activity for a given seismic source (logN(M) for M≥0), and b-value represents the ratio between small and large events. Identification of the completeness magnitude of an earthquake catalog is a clear requirement for the processing of input data for seismic hazard analysis. The complete part of the declustered SHEEC is an input to estimate the spatial and magnitude probability density of seismicity in the region, using the same approach used to obtain the seismicity density for entire Europe (Hiemer et al., 2014). The declustered catalog for our area of study is divided into 0.1 magnitude bin intervals with a minimum magnitude of 4.1 and time bins of 1.0 year starting from 1960. For our study area, the magnitude of completeness Mc = 4.1 from the Gutenberg-Richter relation was obtained based on the maximum curvature method and the goodness-of-fit test on the ZMAP software (Wiemer, 2001), with an estimate of a = 5.83 and b = 0.87 for the entire region of study (Fig. 2c). The b-value obtained in this study is consistent with those by Grünthal et al. (2010), who reported the b-value range from 0.87 to 0.91 for a superzone covering Albania.

3 Earthquake forecasting models

An earthquake source model is an established approach to forecast earthquake occurrences based on seismological, geological, tectonic, and geodetic data, with varying degrees of importance represented in the source typologies. The basic component of the forecasting model is an earthquake source model that determines the rate of earthquake activity, and the rate of occurrence of events as a function of space, time, and magnitude (Hiemer et al., 2014). Here, we propose two forecasting models, the area source and smoothing models, detailed below.

3.1 The area source model

155 Area source models are one of the most implemented approaches to assess seismic hazard, to characterize seismicity that occurs over large regions where single fault structure detection and classification, determination of location, geometry, and seismicity frequency parameters are difficult (Wiemer et al., 2009). Our study area is covered by 20 area source polygons as proposed by ESHM13 (Fig.3a), and those areas with few events have been merged into the areas with similar characteristics. Seismicity activity in the forms of a- and b-values (Gutenberg and Richter, 1944), the annual rate of seismic activity, and the

160 maximum magnitude (Mmax) are evaluated for each of the area sources as given in Table 1.

ID	IDAS	TECTONICS	a	b	Mmax (Inferred)
1	ALAS179	Active Shallow Crust	4.99 (±0.075)		6.3
2	MKAS180	Active Shallow Crust	4.82 (±0.097)		6.9
3	YUAS184	Active Shallow Crust	4.52 (±0.125)		5.9
4	MKAS187	Active Shallow Crust	4.47 (±0.139)		6.2
5	BAAS191	Active Shallow Crust	4.96 (±0.076)		5.7
6	BAAS192	Active Shallow Crust	5.04 (±0.073)		6.0
7	ITAS312	Active Shallow Crust	4.16 (±0.176)		4.8
8	GRAS369	Active Shallow Crust	5.50 (±0.045)		6.6
9	GRAS370	Active Shallow Crust	4.71 (±0.103)		6.2
10	GRAS375	Active Shallow Crust	4.77 (±0.082)		5.9
11	GRAS384	Active Shallow Crust	5.37 (±0.052)	0.87(± 0.03)	6.7
12	GRAS385	Active Shallow Crust	4.47 (±0.125)		6.2
13	GRAS386	Active Shallow Crust	4.79 (±0.079)		6.2
14	GRAS387	Active Shallow Crust	4.82 (±0.090)		6.7
15	GRAS388	Active Shallow Crust	4.74 (±0.090)		6.3
16	HRAS995	Active Shallow Crust	4.92 (±0.078)		6.9
17	ALAS993	Active Shallow Crust	4.82 (±0.090)		5.9
18	ALAS992	Active Shallow Crust	5.17 (±0.062)		6.7
19	YUAS990	Active Shallow Crust	4.91 (±0.055)		6.4
20	GRAS371	Active Shallow Crust	5.06 (±0.055)		7.0

Table 1. Area source parameters for our region of study, and seismicity rate are given in Fig.3. *Area IDAS are the same as those given by ESHM13 for each of the areas (the IDAS of the area with more events is kept over other merged areas).

Since there is an insufficient number of events in some areas to obtain reliable Gutenberg-Richter parameters, we considered

165 a fixed b=0.87±0.03 for the entire region (Fig. 2c), which is used to define the a-value for each of the areas. A uniform b-value

for all the area sources is sometimes implemented by probabilistic seismic hazard assessment, to minimize the effect of zonation and the low number of events inside each individual area (e.g., Fujiwara et al., 2013; Chan et al., 2020). The a-value, which represents the overall activity of the seismic source, is calculated based on the unified b-value (Table 1). The annual rate for each area source is estimated to forecast the number of events with different magnitudes within each of them, and the seismicity rate per km2 is plotted as given in Fig. 3a.

(a)

(b)

Density seismicity rate (/km²/year)
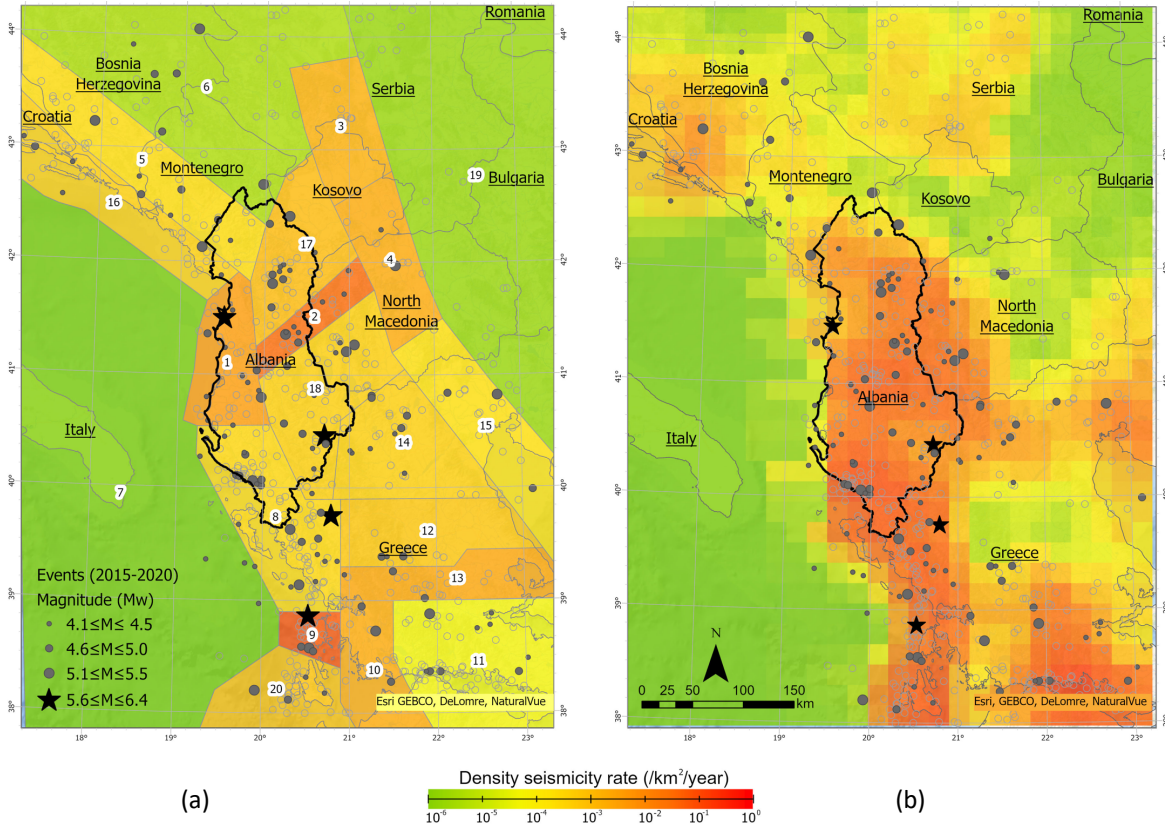
10^{-6} 10^{-5} 10^{-4} 10^{-3} 10^{-2} 10^{-1} 10^{0}

Figure 3: Density seismicity rate for the period 1960–2006 evaluated: a) area source model and b) smoothing model. Stars and gray-filled circles of various sizes represent the events of different magnitudes that occurred during the "testing period" in 2015–2020 (from the IGS catalog). Grey open circles in the background denote the events that occurred during the "learning period" of SHEEC (1960–2006). Numbers represent the ID labels for the area sources as Table 1.

The maximum magnitude (Mmax) for each area was estimated from the maximum observed magnitude in the catalog using the method proposed by Kijko and Sellevoll (1992) and Fundo et al. (2012). As shown in Table 1, the area source GRAS371 (ID20) has the largest maximum magnitude in the catalog with Mmax = 7.0. Duni et al. (2010) for the area including the territory of Albania concluded maximum magnitude Mmax=7.2 and Mmax=6.9 for the historical and instrumental periods, respectively.

3.2 The smoothing model

200   Besides the area source model, another seismogenic source model based on the smoothing kernel as proposed by Frankel (1995) is used for earthquake forecasting. The same approach is used to obtain the smoothed seismicity rates for the Harmonization of Seismic Hazard Maps in the Western Balkan Countries Project (BSHAP, Salic et al., 2018). The method applies a simple isotropic Gaussian smoothing kernel to derive the expected rate of events at each cell from the observed rate of seismicity in a grid of cells with correlation distance c, represented as:

$$\tilde{n}_i = \frac{\sum n_j e^{d_{ij}^2/c^2}}{\sum e^{d_{ij}^2/c^2}} \tag{3}$$

205

where $\tilde{n}_i$ is the expected rate of events at each cell, n_j is the observed rate of seismicity in a grid of j cells, d^{ij} is the distance between the ith and j^{th} cells, and c is the correlation distance for the adaptive kernel. Input parameters are the grid extend and grid cell size, the uniform b-value, bandwidth (in kilometers), completeness magnitude and completeness year, the computed result is the observed number of earthquakes in each cell and smoothed seismicity rate. To apply the method, the area of study

210   is divided into grid cells with a size of 0.2˚x 0.2˚ and the rate of earthquakes ($\tilde{n}_i$) with M≥4.1 is counted for each cell, this count represents the maximum likelihood estimate for that cell based on the method by Weichert (1980). The grid size 0.2˚x 0.2˚ is based on the events location uncertainty as given by ESHM13 at the range of 10 to 15 km (Woessner et al., 2011). To apply the smoothing model, we follow the procedure (code) in Hazard Modeller's Toolkit, an open-source library that is related to the OpenQuake-engine hazard calculation software (Weatherill et al., 2014). In this study, the correlation distance is fixed

215   at 50 km, after testing different bandwidth values, 25 km and 50 km. As indicated in the original work by Frankel (1995), correlation distance larger than 50 km spread out the seismicity so that details are lost and smaller correlation distances resulted in segmented patterns of seismicity. The annual rates from the smoothed model were obtained for both bandwidths, and we show the compared forecasted seismicity rates in Fig.4. The annual rates from the smoothed model for the bandwidth of 50 km (shown in Fig.3b), forecast the highest seismicity rate in the south and west of the study area, where the largest number of

220   events is located and moderate-to-large earthquakes have occurred.
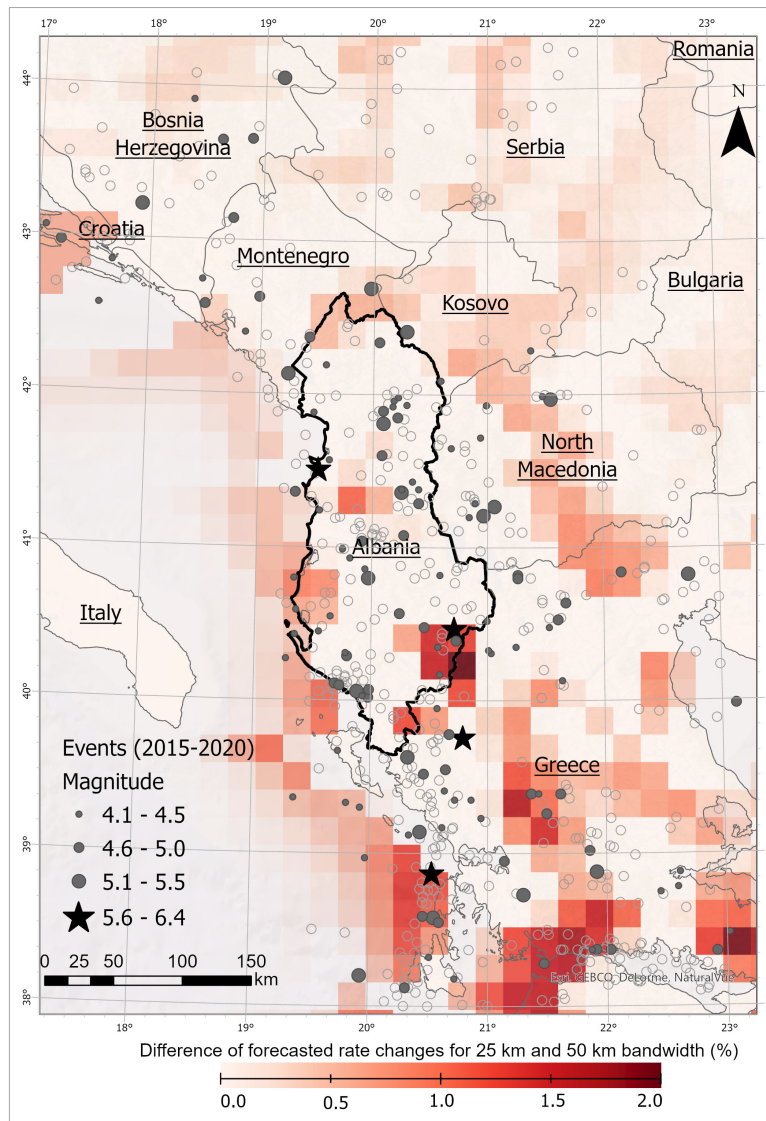
Figure 4: The difference in the forecasted density rate by considering different bandwidths of 25 km and 50 km in the smoothing model. The earthquakes in the "testing period" are shown as stars and grey filed circles, grey open circles denote the events that occurred during the "learning period".

3.3 Model validation

To validate the performance of the models, the Molchan diagram approach is used (Molchan, 1990; Zechar and Jordan, 2008). This method aims to quantify the forecasting ability by investigating the correlation or relationship between a model and observations of earthquake events. After obtaining the seismicity for the area of study from the area source model and the smoothing model, we forecast the spatial distribution of the seismicity during the period of time 2015 – 2020. The data are collected by combining the catalog and the bulletin data from the Institute of Geo-science of Albania (as 'the IGS catalog'),

selecting events with a magnitude larger than the threshold (M≥4.1) represented by gray dots, and events with magnitude M≥5.0 represented by black stars, as shown in Fig. 3. The reported event magnitude from IGS is local magnitude (ML), and

255   the conversion to moment magnitude (Mw) follows the relevant regression equations by Duni et al. (2010):

$$M_w = 1.624 + 0.743 M_L \tag{4}$$

One of the largest events in this period in the territory of Albania is recorded along the coastline, it occurred on November 26, 2019, with Mw6.4, the most destructive earthquake in the western part of the country. The area of study is divided into grid cells 0.2º × 0.2º to obtain and validate the seismicity for each of the catalogs through the area source model and smoothing

260   model. We have defined the catalogs from SHEEC (1960–2006) as the "learning" catalog and the IGS (2015–2020) as the "testing" catalog. Both catalogs were declustered with the same window method by Gardner and Knopoff (1974) for shallow crustal events, and we prefer to follow similar analysis procedures for a better evaluation between our data and models. For the "testing" catalog, we have determined the fraction of alarm-occupied space as the percentage of observations within the region with a forecasting level equal to or higher than "alarm", and the fraction of failure in forecasting as the percentage of

265   observations having a lower forecasting level than "alarm". Since the study region is divided into grid cells, each cell in which an earthquake is forecast to occur constitutes an alarm cell.

A Molchan diagram plots the missing rate versus the alarming rate, and each of them gets a value from 0 to 1 (0% to 100%), if the alarming rate changes from 0 to 1, the missing rate will decrease from 1 to 0. The diagonal line from (0,1) to (1,0) would be the long-run expectation for alarms that are declared randomly, i.e., the missing rate equals the alarming rate, indicating a

270   completely random guess. A perfect forecast would have a value of missing alarm equal to 0 (no false alarms) and an alarm equal to 1, meaning all earthquakes are perfectly forecasted (Molchan, 1990; Molchan, 1991). The prediction points under the diagonal line mean the missing rate is less than the alarming rate and the prediction is better than a random guess, which is consistent with our analysis as they follow the definition given for the evaluation of source models with the Molchan diagram. We underlined that both obtained diagrams show good performance for the targeted observations but are more suitable for

275   large events. Also, the smoothed model indicates a better forecast for future events than the area source model, as the predictive curve is always lower than the area source model's predictive curve. The forecasting performance from different source models is investigated by plotting the curve at a 99% confidence interval of the null hypothesis for the forecasting events with M≥4.1 and M≥5.0 (shown in Figs. 5a and b, respectively), confirming the good forecasting performance of the area source and smoothing model as both respective curves are under the confidence interval curve. As discussed by Schorlemmer et al. (2010),

280   assuming a null hypothesis where the observations fall into the lower curve of the distribution, the null hypothesis is rejected.

Forecasting sesimicity M ≥ 4.1   Forecasting sesimicity M ≥ 5.0

(a)   (b)
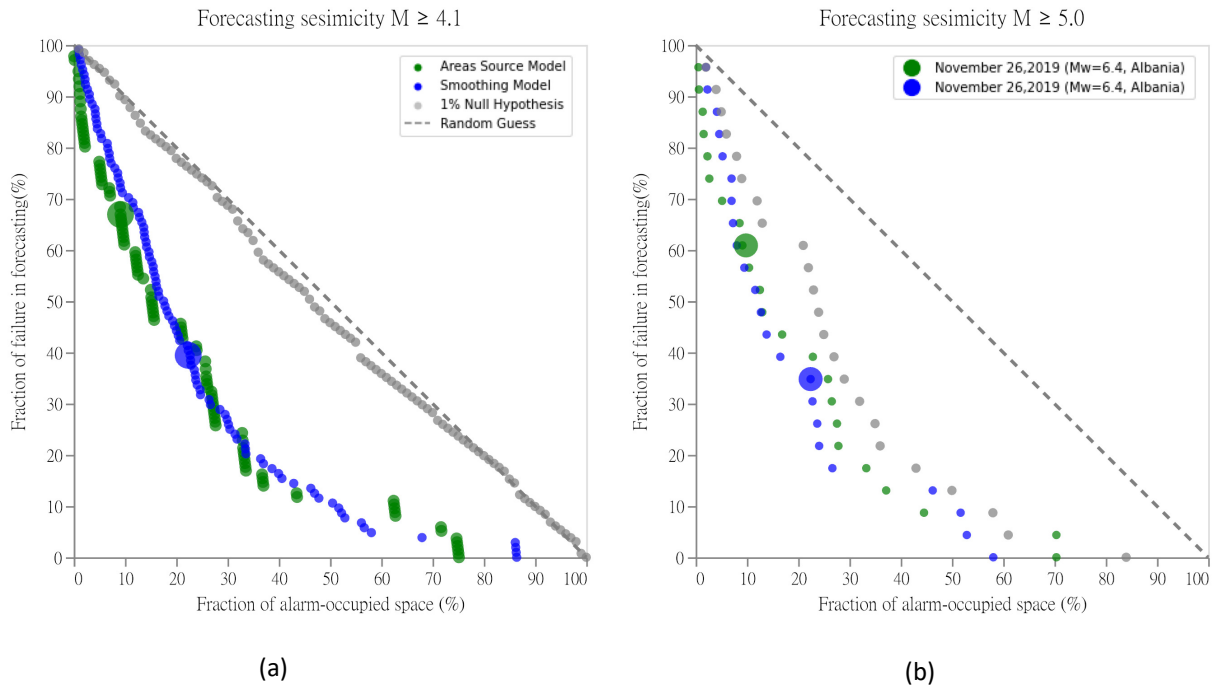
Figure 5: Molchan diagram performance in the IGS catalog during 2015-2020 for (a) the events with M≥4.1, and (b) the events with M≥5.0. The pink dots mark the result from the area source model, and the green dots show the result from the smoothing model. Grey dots denote the 1% null hypothesis for 132 events (M≥4.1) and for 23 events (M≥5.0), respectively. Squares represent the 2019 Mw6.4 event on the diagram for each model.

4 Discussion and conclusions

The present study was designed to propose earthquake forecasting models and to discuss the seismic activity in one of the most seismic regions on the European continent, using past earthquakes to forecast future earthquakes. Two forecasting approaches are used to obtain the spatial distribution of the seismicity rate, considering events with a minimum magnitude of 4.1, which represent the threshold of catalog completeness. The boundary is lower than the minimum magnitude (Mmin = 4.5) considered by Fundo et al. (2012), as the low bound for building damage. The annual seismicity rate for our forecasting models are determined from the complete part of the declustered earthquake catalog, taking into account a- and b-values, and the distribution of maximum magnitude (Mmax). The highest seismicity activity rate is forecasted along the western coastline and southern part of the study region, which corresponds to the location of observed earthquakes as given by the earthquake catalog, compared to the low activity rates in the inner part of the region. The determined seismic rate from the two models, as shown in Fig. 3, is consistent with previous studies that discuss seismicity, as reported by Slejko et al., 1999; Aliaj et al., 2004; Fundo et al., 2012; Salic et al., 2018, and Woessner et al., 2015. To evaluate the smoothing model's uncertainty and the impact of bandwidths, we compared the forecasted seismicity rates corresponding to two different bandwidths of 25 km and 50 km, which are comparable to the events location uncertainty described in Section 3.2. The difference in rate between the two

smoothing models shows that changes are less than 2% for the entire study region, and both models are distinguished by a level of confidence probability greater than 98% (Fig. 4). Note that most of the forecasting events are in the region with the insignificant difference in the seismicity rate. When we compare our models with observations as given by IGS, the higher seismicity rate is highlighted along the coastline (Fig. 3). Maximum magnitude based on the observed events has the value 6.8, which is comparable with Mmax = 6.9, claimed by Duni et al. (2010) as the maximum magnitude for the instrumental period in Albania for the catalog period from 510 BC to 2008 AD, proving that our estimations for Mmax obtained following the method proposed by Kijko and Sellevoll (1992) seem to be reasonable. Furthermore, to test the consistency of the results from the area source and smoothing model, the credibility of our models was confirmed by the Molchan diagram, as all the events from the testing catalog (represented by gray dots and black stars in Figs. 3 and 4) are under the diagonal line, approving the good forecasting ability of both above approaches. The models show better forecasting ability for larger events with M≥5.0 than for smaller ones with M≥4.1 (Fig. 5). Many of the events occur in areas where both earthquake source models have high forecasting rates, and such conclusion is crucial for probabilistic seismic hazard assessment. We present the location of the November 26, 2019 (Mw6.4) event (black stars, in Figs. 3 and 4) that occurred in the western part of Albania on the Molchan diagram, which appears to have a low fraction of alarm-occupied space for the smoothing model, confirming again a better forecasting performance compared to the forecasting performance from the area source model (Fig. 5). Our findings are different from the Taiwan experience (Chan et al., 2018), as the seismicity rates were forecasted using a magnitude-dependent smoothing approach proposed by Woo (1996). On a contrary, the smoothing kernel (Frankel, 1995) we implemented is magnitude-independent, and the spatial distribution of large magnitudes could be forecasted based on the distribution of smaller events, providing better forecasting ability. Findings regarding seismicity parameters and source models as presented above have significant implications for the understanding of seismic activity in our region and to raise awareness of the earthquake phenomenon. Additional studies are desired for further investigation of the earthquake catalog including a longer period, and to integrate supplementary data regarding other seismogenic sources from geological and tectonic information for the subsequent probabilistic seismic hazard assessment. This study can be used for future research works completed with information about the fault activity, segmentation models, rupture process documentation, and seismic moment accumulation which are not incorporated into our forecasting model.

Data availability

The data (catalogs and area polygons) in this study are provided by the European Facilities for Earthquake Hazard and Risk (EFEHR) and are available online through the ESHM13 Overview on http://efehrcms.ethz.ch/en/Documentation/specific-hazard-models/europe/overview/. The SHEEC catalog (1900-2006) was compiled by the German Research Center for Geo-sciences (GFZ, Potsdam) and released under https://www.gfz-potsdam.de/emec/ as part of an independent project, representing a spatial-temporal extract from the "European-Mediterranean Earthquake Catalog (EMEC)". The 2013 Euro-Mediterranean Seismic Hazard Model (ESHM13) was developed within the SHARE Project, and more information can be found at

350 **Acknowledgements**

This study was supported by the Ministry of Science and Technology in Taiwan-under the grants MOST 109-2116-M-008-029-MY3, MOST 110-2124-M-002-008008, and MOST 110-2634-F-008-008. This work is financially supported by the Earthquake Disaster & Risk Evaluation and Management Center (E-DREaM) from the Featured Areas Research Center Program within the framework of the Higher Education Sprout Project by the Ministry of Education in Taiwan. The authors

355 thank the editor, Maria Ana Baptista, the reviewer, Mohammad Mokhtari and one anonymous reviewer for their constructive comments.

References

Aliaj, S., Adams, J., Halchuk, S., Sulstarova, E., Peçi, V., and Muço, B.: Probabilistic seismic hazard maps for Albania, https://doi.org/10.4095/226354, 2004.

Aliaj, S., Kociu, S., Muco, B., and Sulstarova, E.: Seismicity, seismotectonics and seismic hazard assessment in Albania, 2010.

Çağnan, Z. and Kalafat, D.: A New Catalogue of Eastern Mediterranean Earthquakes, 2150 BC – 201, 10, 2012.

Chan, C., Ma, K., Lee, Y., and Wang, Y.: Rethinking Seismic Source Model of Probabilistic Hazard Assessment in Taiwan after the 2018 Hualien, Taiwan, Earthquake Sequence, Seismological Research Letters, 90, 88–96, https://doi.org/10.1785/0220180225, 2018.

Chan, C.-H.: Importance of three-dimensional grids and time-dependent factors for applications of earthquake forecasting models to subduction environments, Natural Hazards and Earth System Sciences, 16, 2177–2187, https://doi.org/10.5194/nhess-16-2177-2016, 2016.

Chan, C.-H., Ma, K.-F., Shyu, J. B., Lee, Y.-T., Wang, Y.-J., Gao, J.-C., Yen, Y.-T., and Rau, R.-J.: Probabilistic seismic hazard assessment for Taiwan: TEM PSHA2020, Earthquake Spectra, 36, 875529302095158, https://doi.org/10.1177/8755293020951587, 2020.

Cornell, C. A.: Engineering seismic risk analysis, Bulletin of the Seismological Society of America, 58, 1583–1606, https://doi.org/10.1785/BSSA0580051583, 1968.

Duni, L., Kuka, S., and Kuka, N.: Local relations for converting M L to M W in Southern-Western Balkan region, Acta Geodaetica Et Geophysica Hungarica - ACTA GEOD GEOPHYS HUNG, 45, 317–323, https://doi.org/10.1556/AGeod.45.2010.3.6, 2010a.

Duni, L., Kuka, N., Kuka, S., and Fundo, A.: Towards a New Seismic Hazard Assessment of Albania, in: 14th European Conference on Earthquake Engineering 2010, 14th European Conference on Earthquake Engineering 2010, Red Hook, NY, 8, 2010b.

Frankel, A.: Mapping Seismic Hazard in the Central and Eastern United States, Seismological Research Letters, 66, 8–21, https://doi.org/10.1785/gssrl.66.4.8, 1995.

Fujiwara, H., Morikawa, N., and Okumura, T.: Seismic Hazard Assessment for Japan: Reconsiderations After the 2011 Tohoku Earthquake, Journal of Disaster Research, 8, 848–860, https://doi.org/10.20965/jdr.2013.p0848, 2013.

Fundo, A., Ll, D., Kuka, S., Begu, E., and Kuka, N.: Probabilistic seismic hazard assessment of Albania, Acta Geodaetica et Geophysica Hungarica, 47, 465–479, https://doi.org/10.1556/ageod.47.2012.4.7, 2012.

Gardner, J. K. and Knopoff, L.: Is the sequence of earthquakes in Southern California, with aftershocks removed, Poissonian?, Bulletin of the Seismological Society of America, 64, 1363–1367, https://doi.org/10.1785/BSSA0640051363, 1974.

Giardini, D.: The Global Seismic Hazard Assessment Program (GSHAP)-1992/1999, Annali di Geofisica, 42, https://doi.org/10.4401/ag-3780, 1999.

Grünthal, G. and Wahlström, R.: The European-Mediterranean Earthquake Catalogue (EMEC) for the last millennium, J Seismol, 16, 535–570, https://doi.org/10.1007/s10950-012-9302-y, 2012a.

Grünthal, G. and Wahlström, R.: The European-Mediterranean Earthquake Catalogue (EMEC) for the last millennium, J Seismol, 16, 535–570, https://doi.org/10.1007/s10950-012-9302-y, 2012b.

Grünthal, G., Arvidsson, R., and Bosse, C.: Earthquake model for the European-Mediterranean Region for the purpose of GEM1, 1–35, https://doi.org/10.2312/GFZ.b103-10043, 2010.

Gutenberg, B. and Richter, C. F.: Frequency of earthquakes in California*, Bulletin of the Seismological Society of America, 34, 185–188, https://doi.org/10.1785/BSSA0340040185, 1944.

Hiemer, S., Woessner, J., Basili, R., Danciu, L., Giardini, D., and Wiemer, S.: A smoothed stochastic earthquake rate model considering seismicity and fault moment release for Europe, Geophysical Journal International, 198, 1159–1172, https://doi.org/10.1093/gji/ggu186, 2014.

Jimenez, J., Giardini, D., and Grunthal, G.: The ESC-SESAME Unified Hazard Model for the European-Mediterranean region, 5, 2003.

Jiménez, M., D.Giardini, Grünthal, G., Erdik, M., García-Fernández, M., J.Lapajne, Makropoulos, K., R.Musson, Papaioannou, C., Rebez, A., Riad, S., Sellami, S., A.Shapira, Slejko, D., Eck, T., and Sayed, A. E.: Unified Seismic Hazard Modeling Throughout The Mediterranean Region, Bollettino di Geofisica Teorica ed Applicata, 3–18, 2001.

Kijko, A. and Sellevoll, M.: Estimation of earthquake hazard parameters from incomplete data files. Part II. Incorporation of magnitude heterogeneity, Bulletin of the Seismological Society of America, 82, 120–134, 1992.

Makropoulos, K., Kaviris, G., and Kouskouna, V.: An updated and extended earthquake catalogue for Greece and adjacent areas since 1900, Natural hazards and earth system sciences, 12, 1425–1430, https://doi.org/10.5194/nhess-12-1425-2012, 2012.

Markušić, S., Gülerce, Z., Kuka, N., Duni, L., Ivančić, I., Radovanović, S., Glavatović, B., Milutinović, Z., Akkar, S., Kovačević, S., Mihaljević, J., and Šalić, R.: An updated and unified earthquake catalogue for the Western Balkan Region, Bull Earthquake Eng, 14, 321–343, https://doi.org/10.1007/s10518-015-9833-z, 2016.

Molchan, G. M.: Strategies in strong earthquake prediction, Physics of the Earth and Planetary Interiors, 61, 84–98, https://doi.org/10.1016/0031-9201(90)90097-H, 1990.

Molchan, G. M.: Structure of optimal strategies in earthquake prediction, Tectonophysics, 193, 267–276, https://doi.org/10.1016/0040-1951(91)90336-Q, 1991.

Muço, B.: Catalogue of ML≥3.0 earthquakes in Albania from 1976 to 1995 and distribution of seismic energy released, Tectonophysics, 292, 311–319, https://doi.org/10.1016/S0040-1951(98)00071-7, 1998.

Muco, B., Kiratzi, A., Sulstarova, E., Kociu, S., Peci, V., and Scordilis, E.: Probabilistic Seismic Hazard assessment in Albania, AGU Fall Meeting Abstracts, 2002.

Muco, B., Alexiev, G., Aliaj, S., Elezi, Z., Grecu, B., Mandrescu, N., Milutinovic, Z., Radulian, M., Ranguelov, B., and Shkupi, D.: Geohazards assessment and mapping of some Balkan countries, NATURAL HAZARDS, 64, 943–981, https://doi.org/10.1007/s11069-012-0185-6, 2012.

Salic, R., Gulerce, Z., Kuka, N., Markušić, S., Mihaljevic, J., Kovačević, V., Sandikkaya, M. A., Milutinovic, Z., Duni, L., Stanko, D., Kaludjerovic, N., and Kovačević, S.: Harmonized seismic hazard maps for the western Balkan countries, in: 16th European Conference on Earthquake Engineering, 16th European Conference on Earthquake Engineering, Thessaloniki, Greece, 2018.

Schorlemmer, D., Zechar, J. D., Werner, M. J., Field, E. H., Jackson, D. D., Jordan, T. H., and the RELM Working Group: First Results of the Regional Earthquake Likelihood Models Experiment, Pure Appl. Geophys., 167, 859–876, https://doi.org/10.1007/s00024-010-0081-5, 2010.

Shebalin, N. V., Karnik, V., and Hadzievski, D.: Catalogue of earthquakes of the Balkan region, 1974.

Slejko, D., Camassi, R., Cecic, I., Muço, B., and Herak, D.: Seismic hazard assessment for Adria, 1999.

Stepp, J. C.: Analysis of Completeness of the Earthquake Sample in the Puget Sound Area and Its Effect on Statistical Estimates of Earthquake Hazard | Resolution Copper Project and Land Exchange Environmental Impact Statement, International Conference on Microzonation, 897–910, 1972.

van Stiphout, T., Zhuang, J., and Marsan, D.: Seismicity declustering, Community Online Resource for Statistical Seismicity Analysis, 25, https://doi.org/10.5078/corssa52382934, 2012.

Sulstarova, E.: Earthquake hazard assessment in Albania, in: Risque, nature et société : Actes du séminaire « Delphes I », edited by: Faugères, L. and Villain-Gandossi, C., Éditions de la Sorbonne, Paris, 199–216, 1996.

Weatherill, G., Rodríguez, L., and Pagani, M.: The seismic hazard modeller's toolkit: An open-source library for the construction of probabilistic seismic hazard models, 2014.

Weichert, D. H.: Estimation of the earthquake recurrence parameters for unequal observation periods for different magnitudes, Bulletin of the Seismological Society of America, 70, 1337–1346, https://doi.org/10.1785/BSSA0700041337, 1980.

Wiemer, S.: A Software Package to Analyze Seismicity: ZMAP, Seismological Research Letters, 72, 373–382, https://doi.org/10.1785/gssrl.72.3.373, 2001.

Wiemer, S., García-Fernández, M., and Burg, J.-P.: Development of a seismic source model for probabilistic seismic hazard assessment of nuclear power plant sites in Switzerland: the view from PEGASOS Expert Group 4 (EG1d), Swiss J. Geosci., 102, 189–209, https://doi.org/10.1007/s00015-009-1311-7, 2009.

Woessner, J., Danciu, L., Kästli, P., and Monelli, D.: D6.6 – Databases of seismogenic zones, Mmax, earthquake activity rates, ground motion attenuation relations and associated logic trees, 2011.

Woessner, J., Laurentiu, D., Giardini, D., Crowley, H., Cotton, F., Grünthal, G., Valensise, G., Arvidsson, R., Basili, R., Demircioglu, M. B., Hiemer, S., Meletti, C., Musson, R. W., Rovida, A. N., Sesetyan, K., and Stucchi, M.: The 2013 European Seismic Hazard Model: key components and results, Bull Earthquake Eng, 13, 3553–3596, https://doi.org/10.1007/s10518-015-9795-1, 2015.

Woo, G.: Kernel estimation methods for seismic hazard area source modeling, Bulletin of the Seismological Society of America, 86, 353–362, https://doi.org/10.1785/BSSA0860020353, 1996.

Zechar, J. D. and Jordan, T. H.: Testing alarm-based earthquake predictions, Geophysical Journal International, 172, 715–724, https://doi.org/10.1111/j.1365-246X.2007.03676.x, 2008.

Zhuang, J., Ogata, Y., and Vere-Jones, D.: Stochastic Declustering of Space-Time Earthquake Occurrences, Journal of the American Statistical Association, 97, 369–380, https://doi.org/10.1198/016214502760046925, 2002.

360